A cutting force model for rotary ultrasonic machining of brittle materials

DeFu Liu, W.L. Cong, Z.J. Pei, YongJun Tang

Digital Object Identifier (DOI): doi:10.1016/j.ijmachtools.2011.09.006

Publisher's Link: www.elsevier.com/locate/ijmactool

A Cutting Force Model for Rotary Ultrasonic Machining of Brittle Materials

DeFu Liu[a] , W.L. Cong[b], Z.J. Pei[b, 1], YongJun Tang[c]

[a] College of Mechanical and Electrical Engineering, Central South University, Changsha, Hunan 410083, China

[b] Department of Industrial and Manufacturing Systems Engineering, Kansas State University, Manhattan, KS 66506, USA

[c] Faculty of Electromechanical Engineering, Guangdong University of Technology, Guangzhou, Guangdong 510006, China

Abstract: Knowing cutting force in rotary ultrasonic machining (RUM) can help optimizing input variables. RUM of brittle materials has been investigated both experimentally and theoretically. However, there are no reports on cutting force models for RUM of brittle materials. This paper presents a mechanistic model for cutting force in RUM of brittle materials. Assuming that brittle fracture is the primary mechanism of material removal in RUM of brittle materials, the cutting force model is developed step by step. On the basis of this mechanistic model, relationships between cutting force and input variables (such as spindle speed, feed rate, ultrasonic vibration amplitude, abrasive size, and abrasive concentration) are predicted.

[1] Corresponding author. Tel: +1 785 532 3436; Fax: +1 785 532 3738; Email: zpei@ksu.edu (ZJ Pei)

Experiments are conducted for model verification and experimental results agree well with model predictions.

Keywords: Brittle material; Ceramic; Cutting force; Drilling; Predictive model; Rotary ultrasonic machining

1. Introduction

Superior properties of some brittle materials, such as high hardness and strength at elevated temperatures, chemical stability, low friction, and high wear resistance, make them attractive for many applications. Machining of brittle materials has gained significant importance over the last two decades [1-10]. Rotary ultrasonic machining (RUM) shown in

Fig. 1 is a non-traditional machining process and has been used for brittle materials such as glass [11-12], KDP [13], and ceramics [14]. It is a hybrid process that combines material removal mechanisms of grinding and ultrasonic machining [3]. The rotary core drill with abrasive particles can oscillate at high frequency (typically 20 kHz) while being fed towards the work-piece.

Although there have been some models [14-19] of RUM, most of them were developed for predicting material removal rate (*MRR*) or investigating material removal mechanism, and only one cutting force model for RUM of ductile materials was reported [20]. At present, no publications are available on cutting force models for RUM of brittle materials. Therefore, it is necessary to develop a cutting force model for RUM of brittle materials to help optimizing input

variables.

In this paper, a mechanistic model to predict relations between cutting force and input variables for RUM of brittle materials is developed based on the indentation fracture mechanics under pyramidal indenters. In this mechanistic model, a proportionality parameter will be used to describe the ratio between the actual volume of material removed by one abrasive particle in a vibration cycle and the theoretical volume of the fracture zone induced by the abrasive particle. The model is mechanistic in the sense that this parameter for a particular work-piece material is a constant and can be obtained from a few experiments and then used in prediction of cutting force over a wide range of input variables.

The paper is organized into six sections. Following this introduction section, Section 2 describes the cutting force model development step by step. In Section 3, the proportionality parameter for alumina is obtained by experiments. In Section 4, predicted influences of input variables (such as spindle speed, feed rate, ultrasonic vibration amplitude, abrasive size, and abrasive concentration) on cutting force are discussed. Section 5 provides model verification using pilot experiments. Conclusions are contained in Section 6.

2. Development of Cutting Force Model

2.1. Approach to Model Development

RUM might be considered as a combination of ultrasonic machining process and grinding process [3]. It is a complex process with a large number of input variables, as shown in

Fig. 2. Many abrasive machining models [17-24] began with an analysis of one abrasive particle. The models were then derived by summing up the effects of all active abrasive particles taking part in cutting. A similar approach is used in this paper to develop the cutting force model for RUM of brittle materials. To develop the model, the following steps are carried out:

(1) Establish a relation between cutting force and maximum depth that abrasive particles penetrate into the work-piece.

(2) Estimate *V*, the actual volume of material removed by one abrasive particle in a single ultrasonic vibration cycle.

(3) Establish a cutting force model by aggregating the effects of all active abrasive particles.

Several major assumptions and simplifications on abrasive particles are as following:

(1) The diamond abrasive particles are assumed to be rigid octahedrons of the same size. Some researchers [14-20] took diamond abrasive particles as spheres (like blunt indenters). However, diamond abrasive particles are more like polyhedron in shape (like sharp indenters). Indentation crack patterns are different between “blunt” and “sharp” indenters [25-26]. In order to establish a more accurate model in this paper, diamond abrasive particles are taken as octahedrons instead of spheres. Every four adjacent triangles have a common vertex, forming a pyramid, as shown in

Fig. 3. Only one pyramid of each octahedral particle takes part in cutting.

(2) The semi-angle (β) between two opposite edges of an abrasive particle, as shown in Fog. 3, is 45° before it wears down. Since the lengths of its 12 edges are assumed to be the same (regular octahedron), the size of an abrasive particle (S_a) can be expressed by the length of its

edges. If an abrasive particle wears down (by attritious wear not grain fracture), its semi-angle will increase.

(3) All diamond abrasive particles on the end face of a core drill have the same height and all of them take part in cutting during each ultrasonic cycle.

Other assumptions and simplifications will be presented later when they are used.

2.2. Relation between Cutting Force and Maximum Penetration Depth

When a core drill feeds into the work-piece during RUM, an abrasive particle on the end face of the core drill is not in continuous contact with the work-piece due to ultrasonic vibration of the drill. In each ultrasonic cycle, the abrasive particle on the end face of the core drill will make contact with the work-piece for a certain period of time (Δt - effective cutting time). The maximum impact force between the abrasive particle and the work-piece is produced while the penetration of the active abrasive particle reaches the maximum depth.

If w is the maximum depth that an abrasive particle penetrates into the work-piece, as shown in

Fig. 4, then, according to the definition of Vickers hardness, w can be calculated approximatively by the following equation [25],

$$w = \frac{d}{2\tan\beta} = \left(\frac{1}{2\tan\beta\sqrt{\tan^2\beta + 2}}\frac{F_n}{H_V}\right)^{\frac{1}{2}} \quad (1)$$

where,

w - maximum penetration depth of an abrasive particle, mm;

F_n - maximum impact force applied to one abrasive particle, N;

H_V - Vickers hardness of the work-piece material, MPa;

d - length of the diagonal of indentation, mm, as shown in

Fig. 4.

β - semi-angle between two opposite edges of an abrasive particle.

F_n can be obtained by the following equation,

$$F_n = \frac{F_m}{N_a} \tag{2}$$

where,

F_m – maximum impact force between a core drill and work-piece, N;

N_a - number of active abrasive particles on the end face of a core drill.

The number of abrasive particles on the end face of a core drill can be obtained according to the definition of abrasive concentration. The abrasive concentration is defined by a formula based on weight of abrasives. If the abrasive concentration is 100, then there is 0.88×10^{-3}g of abrasive particles per cubic mm volume (or 72 carats of abrasive particles per cubic inch volume). Since abrasive particle is simplified as a regular octahedron, the volume of an abrasive particle is $\sqrt{2}S_a^3/3$. It is assumed that abrasive particles distribute uniformly in the abrasive portion of a core drill, so the number of active abrasive particles on the end face of core drill can be determined by the following equation,

$$N_a = \left(\frac{0.88 \times 10^{-3}}{\frac{\sqrt{2}}{3} S_a^3 \rho} \cdot \frac{C_a}{100} \right)^{\frac{2}{3}} A_0 = C_1 \frac{C_a^{\frac{2}{3}} A_0}{S_a^2} \tag{3}$$

where,

C_a - abrasive concentration;

S_a - abrasive size, mm, as shown in

Fig. 3;

A_0 - area of the core drill end face, $A_0 = \pi(D_o^2 - D_i^2)/4$, mm^2;

D_o and D_i - outer and inner diameters of the core drill, respectively, mm, as shown in

Fig. 1;

ρ - density of abrasive material, g/mm^3, $\rho = 3.52\times10^{-3}$g/mm^3 for diamond;

C_1 - a dimensionless constant, $C_1 = [3\times0.88\times10^{-3}/(100\sqrt{2}\rho)]^{2/3}=3\times10^{-2}$.

The cutting force (F) measured during the experiments in RUM is not the same as the maximum impact force (F_m). The relation between F and F_m can be approximately derived by equaling the impulse in terms of F to the impulse in terms of F_m during each vibration cycle. This practice to obtain the relation between F and F_m was used in several RUM modeling papers [14, 16, 20].

Since it is assumed that the abrasive particles are rigid, the impulse in terms of the maximum impact force F_m during one cycle of ultrasonic vibration is approximately

$$Impulse = \int_{\text{cycle}} F_m \mathrm{d}t \approx F_m \Delta t \tag{4}$$

where,

Δt - period of time during which an abrasive particle penetrates into the work-piece. It is also called effective cutting time, second (s).

The abrasive particles on the end face of a core drill oscillate with amplitude A and

frequency *f*. Their motions are sinusoidal. The position of each abrasive particle in the *z* direction (the tool axial direction) relative to its mean position can be described by the following equation,

$$z = A\sin(2\pi f t) \tag{5}$$

where,

A - amplitude of the ultrasonic vibration, mm;

f - frequency of the ultrasonic vibration, Hz.

As shown in

Fig. 5, it will take an abrasive particle $\Delta t/2$ to move from $z = (A\text{-}w)$ to $z = A$. Δt can be calculated using the following equation,

$$\Delta t = \frac{1}{\pi f}\left[\frac{\pi}{2} - \arcsin\left(1 - \frac{w}{A}\right)\right] \tag{6}$$

The impulse in terms of the cutting force during one cycle of ultrasonic vibration is

$$Impulse = \frac{1}{f}F \tag{7}$$

where,

F - cutting force measured during the experiments in RUM of brittle materials, N.

By equating the two impulses in Equations (4) and (7), the relation between *F* and F_m can be obtained,

$$F = \Delta t f \quad F_m \tag{8}$$

Substituting Equations (2) and (6) into Equation (8), the relation between *F* and F_n can be described by the following equation,

$$F = \frac{N_a}{\pi}\left[\frac{\pi}{2} - \arcsin\left(1 - \frac{w}{A}\right)\right] F_n \tag{9}$$

By substituting Equation (9) into Equation (1), the relation between the cutting force (*F*)

and the maximum penetration depth (w) can be described by the following equation,

$$w = \left(\frac{F}{2\tan\beta\sqrt{\tan^2\beta + 2}\left[\frac{1}{2} - \frac{1}{\pi}\arcsin\left(1 - \frac{w}{A}\right)\right] H_V N_a} \right)^{\frac{1}{2}} \tag{10}$$

2.3. Volume of Material Removed by One Abrasive Particle

Material removal mechanism in RUM of brittle materials has been mainly attributed to brittle fracture in the literature [14, 17-19, 23-24]. The brittle fracture mechanism of materials has been discussed using indentation fracture mechanics [25-28].

Fig. 4 shows the cracks in brittle materials induced by indentation of an abrasive particle. Lateral crack length C_L and lateral crack depth C_h were given by Marshall *etc*. [28],

$$C_L = C_2 \left(\frac{1}{\tan\beta}\right)^{\frac{5}{12}} \left(\frac{E^{\frac{3}{4}}}{H_V K_{IC} (1 - \nu^2)^{\frac{1}{2}}} \right)^{\frac{1}{2}} (F_n)^{\frac{5}{8}} \tag{11}$$

$$C_h = C_2 \left(\frac{1}{\tan\beta}\right)^{\frac{1}{3}} \frac{E^{\frac{1}{2}}}{H_V} (F_n)^{\frac{1}{2}} \tag{12}$$

where,

C_L - lateral crack length, mm;

C_h - lateral crack depth, mm;

K_{IC} - fracture toughness of the work-piece material, $\mathrm{MPa}\sqrt{\mathrm{mm}}$;

E - Young's modulus of the work-piece material, MPa;

υ - Poisson's ratio of the work-piece material;

F_n - load applied to the abrasive particle, N;

C_2 - a dimensionless constant, independent of material/indenter system, C_2 = 0.226 [28].

As abrasive particles rotate together with the core drill and impact the work-piece due to ultrasonic vibration, the material on work-piece surface is removed by propagation and intersection of cracks. In this paper, the actual volume (V) of material removed by one abrasive particle in a vibration cycle is assumed to be proportional to the theoretical volume (V_0) of fracture zone induced by one abrasive particle in an ultrasonic vibration cycle.

Fig. 6 illustrates how to calculate the volume of fracture zone (V_0). L_s is effective cutting distance that an abrasive particle travels during effective cutting time Δt. It can be calculated from the following equation,

$$L_s = \frac{2\pi SR}{60}\Delta t \tag{13}$$

where,

R - distance of the abrasive particle to the center of the core drill, mm;

S - spindle speed, rpm.

During the period of time Δt, the penetration of the abrasive particle increases from 0 to w and decreases to 0 while the abrasive particle moves through L_s on the work-piece surface. As a result, the length and width of the lateral crack will also increase from zero to their maximum values and decrease to zero. As shown in

Fig. 6, the fracture zone can be simplified as 2 times the volume of tetrahedron $ABCD$,

$$V_0 = 2 \cdot V_{ABCD} = \frac{1}{3} C_L C_h L_s \tag{14}$$

Due to interrelations among abrasive particles during RUM, there exist some differences between the actual volume (V) of material removed by one abrasive particle in a vibration cycle

and the theoretical volume (V_0) of fracture zone. In this paper, V is assumed to be proportional to V_0, with a constant proportionality parameter, K. The actual volume of material removed by one abrasive particle in an ultrasonic vibration cycle can be expressed as,

$$V = KV_0 = \frac{K}{3} C_L C_h L_s = \frac{\pi}{90} K C_L C_h S R \Delta t \tag{15}$$

where,

K - a proportionality parameter which is assumed to be constant for a given work-piece material over a wide range of input variables. The value of K can be obtained from RUM experiments.

2.4. Cutting Force Model

Material removal rate of one abrasive particle (MRR_a) can be theoretically calculated from the product of the actual volume (V) of material removed by one abrasive particle in an ultrasonic vibration cycle and the vibration frequency (f). By substituting equation (6) into equation (15), MRR_a is described by the following equation,

$$MRR_a = fV = \frac{K}{90} C_L C_h S R \left[\frac{\pi}{2} - \arcsin\left(1 - \frac{w}{A}\right)\right] \tag{16}$$

Material removal rate of a core drill (MRR_T) can be obtained from the summation of MRR_a of all abrasive particles on the end face of the core drill. To simplify calculation, the distance of each abrasive particle to the center of the core drill (R) can be replaced by their average distance to the center of the core drill. Hence, MRR_T can be described by the following equation,

$$MRR_T = N_a \cdot MRR_a = N_a f V \approx \frac{K}{90} C_L C_h S N_a \frac{(D_o + D_i)}{4} \left[\frac{\pi}{2} - \arcsin\left(1 - \frac{w}{A}\right)\right] \tag{17}$$

In addition, MRR_T can also be expressed in terms of the feed rate and the area of the core drill end face,

$$MRR_T = f_r A_0 = \frac{\pi(D_o^2 - D_i^2)}{4} f_r \tag{18}$$

where,

f_r - the feed rate during RUM, mm/s.

By equating Equations (17) and (18), and substituting Equations (11) and (12) into Equation (17), the relation between cutting force (F) and input variables can be obtained by the following equation,

$$KC_3 S(D_o + D_i)\left(\frac{1}{\tan\beta}\right)^{\frac{3}{4}}\left(\frac{E^{\frac{7}{4}}}{H_V^3 K_{IC}(1-\nu^2)^{\frac{1}{2}}}\right)^{\frac{1}{2}}\left(\frac{1}{N_a\left[\frac{\pi}{2} - \arcsin\left(1 - \frac{w}{A}\right)\right]}\right)^{\frac{1}{8}} F^{\frac{9}{8}} = f_r A_0 \tag{19}$$

where,

C_3 - a dimensionless constant, $C_3 = \pi^{9/8}(C_2)^2/360 = 5.15\times10^{-4}$.

F and w are two unknown terms in Equation (19) if K is obtained by experiments. Another relation between F and w has already been described by Equation (10). So, cutting force (F) and maximum penetration depth (w) can be obtained by solving Equations (10) and (19) simultaneously.

3. Obtaining proportionality parameter *K*

3.1. Experimental Setup

Rotary ultrasonic machining experiments are performed on a machine of Sonic Mill Series 10 (Sonic-Mill, Albuquerque, NM, USA). The experimental setup mainly consists of an ultrasonic spindle system, a data acquisition system, and a coolant system. The ultrasonic spindle

system comprises of an ultrasonic spindle, a power supply, and a motor speed controller. The power supply converts 60 Hz electrical supply to high frequency (20 kHz) AC output. This is fed to the piezoelectric transducer located in the ultrasonic spindle. The ultrasonic transducer converts electrical input into mechanical vibrations. The motor attached atop the ultrasonic spindle supplies the rotating motion of the core drill and different speeds can be obtained by adjusting the motor speed controller. The fixture to hold the specimen is mounted on a dynamometer that is attached to the machine table. The cutting force along feed direction is measured by Kistler 9272 piezoelctric dynamometer produced by Kistler Instrument Corporation. The electrical signals from the dynamometer are transformed into numerical signals by an A/D converter. Then the numerical signals are displayed and saved on the computer with the help of National Instruments LabVIEW^{TM}. Sampling frequency to obtain the cutting force signals is 20 Hz. The core drills with metal-bond diamond abrasive particles are provided by N.B.R. Diamond Tool Corp. (LaGrangeville, NY, USA). The identifications and properties of these drills are listed Table 1.

3.2. Design of Experiments

The work-piece material is alumina. Mechanical properties of the work-piece material are as follows: Elastic modulus E = 390000 MPa, Poisson's ratio ν = 0.24, Vickers hardness H_V = 15200 MPa, Fracture toughness K_{IC} = 142.3 MPa·mm$^{1/2}$ [29].

If K is independent of input variables, as assumed in the model development, then theoretically only one experiment is needed to get its value. However, to verify whether it is

indeed independent of input variables, a number of different experiments for various combinations of input variables are needed. The experimental design is shown in Table 2. The experiments involve five groups of input variables (spindle speed, feed rate, vibration amplitude, abrasive size, and area of core drill end face). Using core drills with different diameters can result in different areas of the core drill end face, and hence different numbers of active abrasive particles on the end face. The following variables are held constant during all test runs.

- Ultrasonic vibration frequency: f = 20 kHz;
- Abrasive: Diamond;
- Abrasive bond type: Metal-bond;
- Abrasive concentration: C_a = 100.

3.3. Analysis of Experimental Results

The purpose of this section is to estimate the value of K for the given work-piece material using the data obtained from the experiments. For each test, one value of K is obtained using measured data of MRR and cutting force. MRR values are used to calculate V using Equation (17), and measured values of cutting force are used to calculate V_0 using Equation (14). These V and V_0 values are plotted together, as shown in

Fig. 7. The slope of least-squares regression line passing through the origin is the estimated K value. The value of K for the overall data is 0.295.

Fig. 8 shows the values of K estimated for each experimental group. It is seen that there are not strong correlations between the values of K and input variables. Though there are some

deviations among these data, one can state that the assumption of K being constant for a particular material is reasonable and the value can be applied to evaluate the cutting force for a given material over a range of input variables.

4. Predicted Influences of Input Variables on Cutting Force

In the previous sections, a mechanistic model for cutting force in rotary ultrasonic machining of brittle materials has been developed. In this section, influences of individual input variables on cutting force in RUM will be predicted using this model. The work-piece material used for such predictions is alumina. The value of K is taken as 0.295. Throughout the calculation, the outer and inner diameters of the core drill are 9.6 mm and 7.8 mm, respectively.

The predicted relations between cutting force and spindle speed, feed rate, ultrasonic vibration amplitude, abrasive size, abrasive concentration are plotted in Figs. 9-13, respectively. It can be seen from these figures that cutting force decreases nonlinearly with spindle speed, and increases approximately linearly with feed rate. However, one also can observe that cutting force varies slightly as vibration amplitude, abrasive size, and abrasive concentration change. Hence, spindle speed and feed rate have significant effects on cutting force in RUM of brittle materials, while ultrasonic vibration amplitude, abrasive size, and abrasive concentration have less significant effects on cutting force.

Fig. 14 shows the predicted relation between cutting force and semi-angle (β) of abrasive particle. It can be seen that cutting force increases noticeably as semi-angle of abrasive particle increases. Increasing of semi-angle means that abrasive particles wear down (by attritious wear).

Therefore, the reason why cutting force increases as abrasive particles wear down can be reasonably explained by the cutting force model.

5. Pilot Experimental Verification

The same experimental setup shown in Section 3 is used for pilot experiments of model verification. To verify the mechanistic cutting force model, a total of 12 experiments are performed by varying each variable for six levels keeping other variables constant as shown in Table 3. Experimental and predicted cutting force values are compared in

Fig. 15. It can be seen that the trends of predicted influences of input variables (spindle speed, feed rate) agree well with the trends determined experimentally.

6. Conclusions

A physics-based cutting force model for rotary ultrasonic machining (RUM) of brittle materials has been developed. The model is used to predict the influences of input variables on cutting force. These predicted influences are compared with those determined experimentally. The trends of predicted influences of input variables on cutting force agree well with the trends determined experimentally. These predicted trends are: (1) cutting force will increase as abrasive concentration, semi-angle of abrasive particle, and feed rate increase and (2) it will decrease as abrasive size, vibration amplitude, and spindle speed increase.

This model is the first cutting force model for RUM of brittle materials in the literature. It

can serve as a useful springboard for development of more sophisticated cutting force models (such as those that consider the dynamic force in the process) and models to predict cutting temperature, tool wear, and surface roughness in RUM.

Acknowledgements

The authors would like to thank National Science Foundation (Grant CMMI-0900462) and China Scholarship Council for their support to this work. The authors gratefully extend their acknowledgements to Sonic-Mill Corporation for supplying the RUM equipment and NBR Diamond Tool Corporation for providing core drills.

References

[1] I.P. Tuersley, A. Jawaid, I.R. Pashby. Review: Various methods of machining advanced ceramic materials, Journal of Materials Processing Technology 42 (4) (1994) 377-390.

[2] M. Komaraiah, P. Narasimha Reddy, Rotary ultrasonic machining- a new cutting process and its performances, International Journal of Production Research 29 (11) (1991) 2177-2187.

[3] D. Prabhakar, P.M. Ferreira, M. Haselkorn, An experimental investigation of material removal rates in rotary ultrasonic machining, Transactions of the North American

Manufacturing Research Institution of SME, Pullman, Washington, USA, May 20-22, Vol. XX, 1992, pp. 211-218.

[4] Z.J. Pei, N. Khanna, P.M. Ferreira, Rotary ultrasonic machining of structural ceramics - A review, Ceramic Engineering and Science Proceedings 16 (1) (1995) 259-278.

[5] T.B. Thoe, D.K. Aspinwall, M.L.H. Wise, Review on ultrasonic machining, International Journal of Machine Tools and Manufacture 38 (4) (1998) 239-255.

[6] N.M. Abbas, D. G. Solomon, M.F. Bahari, A review on current research trends in electrical discharge machining (EDM), International Journal of Machine Tools and Manufacture 47 (7-8) (2007) 1214-1228.

[7] M.M. Islam, A.S. Kumar, S. Balakumar, H.S. Lim, M. Rahman, Characterization of ELID grinding process for machining silicon wafers, Journal of Materials Processing Technology 198 (1-3) (2008) 281-290.

[8] D.E. Brehl, T.A. Dow, Review of vibration-assisted machining, Precision Engineering 32 (3) (2008) 153-172.

[9] A.N. Samant, N.B. Dahotre, Laser machining of structural ceramics—A review, Journal of the European Ceramic Society 29 (6) (2009) 969-993.

[10] M.A. Azmir, A.K. Ahsan, A study of abrasive water jet machining process on glass/epoxy composite laminate, Journal of Materials Processing Technology 209 (20) (2009) 6168-6173.

[11] K.L. Kuo, A study of glass milling using rotary ultrasonic machining, Key Engineering Materials 364-366 (2007) 624-628.

[12] H. Gong, F.Z. Fang, X.T. Hu, Kinematic view of tool life in rotary ultrasonic side milling of hard brittle materials, International Journal of Machine Tools and Manufacture 50 (2010) 303-307.

[13] Q.G. Wang, W.L. Cong, Z.J. Pei, H. Gao, R.K. Kang, Rotary ultrasonic machining of potassium dihydrogen phosphate (KDP) crystal: An experimental investigation on surface roughness, Journal of Manufacturing Processes 11 (1) (2009) 66-73.

[14] Z.J. Pei, D. Prabhakar, P. M. Ferreira, A mechanistic approach to the prediction of material removal rates in rotary ultrasonic machining, Journal of Manufacturing Science and Engineering ASME 64 (1993) 771-784.

[15] Z.J. Pei, P.M. Ferreira, M. Haselkom, Plastic flow in rotary ultrasonic machining of ceramics, Journal of Materials Processing Technology 48 (1995) 771-777.

[16] Z.J. Pei, P.M. Ferreira, Modeling of ductile-mode material removal in rotary ultrasonic machining, International Journal of Machine Tools and Manufacture 38 (1998) 1399-1418.

[17] Q.H. Zhang, C.L. Wu, J.L Sun, Z.X. Jia, The Mechanism of material removal in ultrasonic drilling of engineering ceramics, Proceedings of the Institution of Mechanical Engineers, Part B: Journal of Engineering Manufacture 214 (9) (2000) 805-810.

[18] G. Ya, H.W. Qin, S.C. Yang, Y.W. Xu, Analysis of the rotary ultrasonic machining mechanism, Journal of Materials Processing Technology 129 (2002) 182-185.

[19] C.L. Chao, W.C. Chou, C.W. Chao, C.C. Chen, Material removal mechanisms involved in rotary ultrasonic machining of brittle materials, Key Engineering Materials 329 (2007) 391-396.

[20] N. Qin, Z.J. Pei, C. Treadwell, D.M. Guo, Physics-based predictive cutting force model in ultrasonic-vibration-assisted grinding for titanium drilling, Journal of Manufacturing Science and Engineering ASME 131 (2009) 111-119.

[21] M. U.S. Patnaik Durgumahanti, V. Singh, P. Venkateswara Rao, A New Model for Grinding Force Prediction and Analysis, International Journal of Machine Tools and Manufacture (50) (3) (2010) 231-240.

[22] S. Agarwal, P.V. Rao, Modeling and prediction of surface roughness in ceramic grinding, International Journal of Machine Tools and Manufacture (50) (12) (2010) 1065-1076.

[23] M. Komaraiah, P. Narasimha Reddy, A study on the influence of workpiece properties in ultrasonic machining, International Journal of Machine Tools and Manufacture 33 (3) (1993) 495-505.

[24] Q.H. Zhang, J.H. Zhang, Z.X. Jia, J.L. Sun, Material-removal-rate Analysis in the Ultrasonic Machining of Engineering Ceramics, Journal of Materials Processing Technology 88 (1999) 180-184.

[25] B. Lawn, R. Wilshaw, Review indentation fracture: principles and applications, Journal of Materials Science 10 (1975) 1049-1081.

[26] P. Ostojic, R. Mcpherson, A review of indentation of fracture: its development, principles and limitations, International Journal of Fracture 33 (1987) 297-312.

[27] B.R. Lawn, A.G. Evans, D.B. Marshall, Elastic/plastic indentation damage in ceramics: The median/radial crack system, Journal of the American Ceramic Society 63 (9-10) (1980) 574-581.

[28] D.B. Marshall, B.R. Lawn, A.G. Evans, Elastic/plastic indentation damage in ceramics: The lateral crack system, Journal of the American Ceramic Society 65 (11) (1982) 561-566.

[29] W. Zhang, G. Subhash, An elastic-plastic-cracking model for finite element analysis of indentation cracking in brittle materials, International Journal of Solids and Structures 38 (2001) 5893-5913.

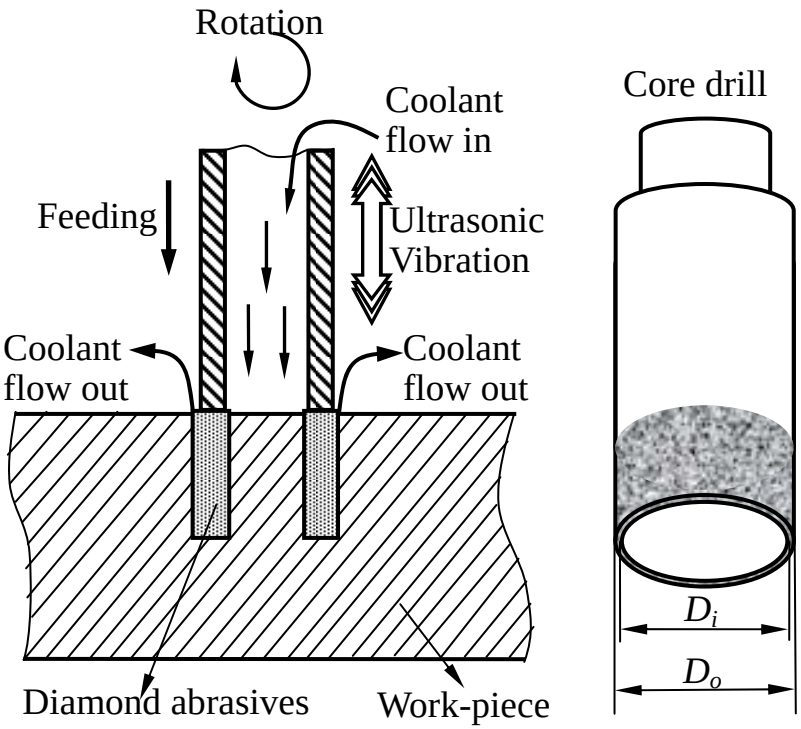

Fig. 1. Illustration of RUM process (after [3]).

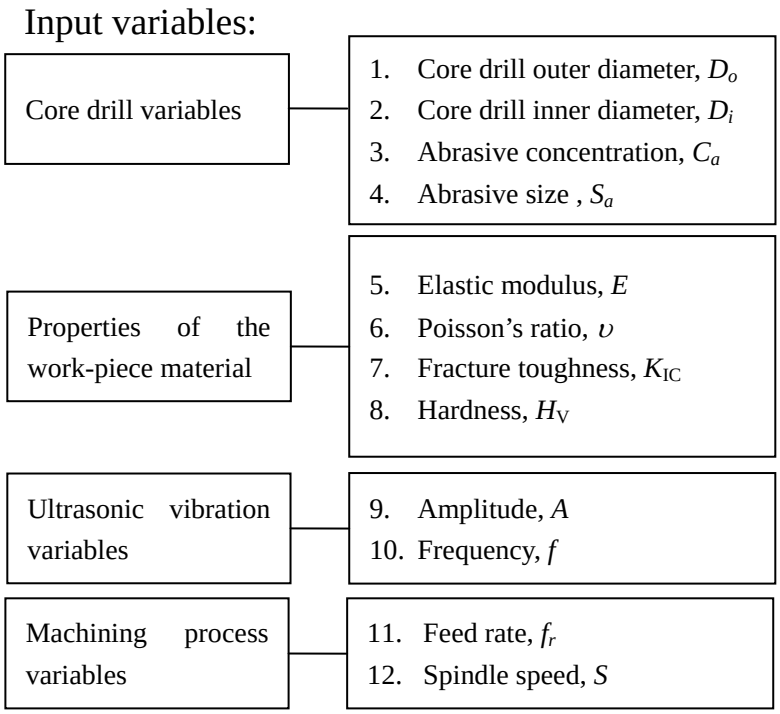

Fig. 2. Input variables in development of cutting force model for RUM.

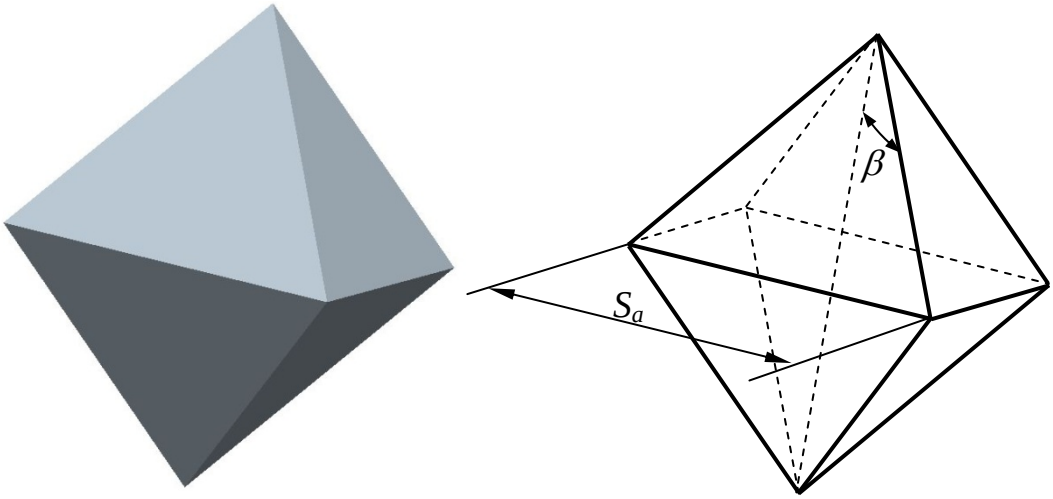

Fig. 3. Illustration of abrasive particle simplified as an octahedron.

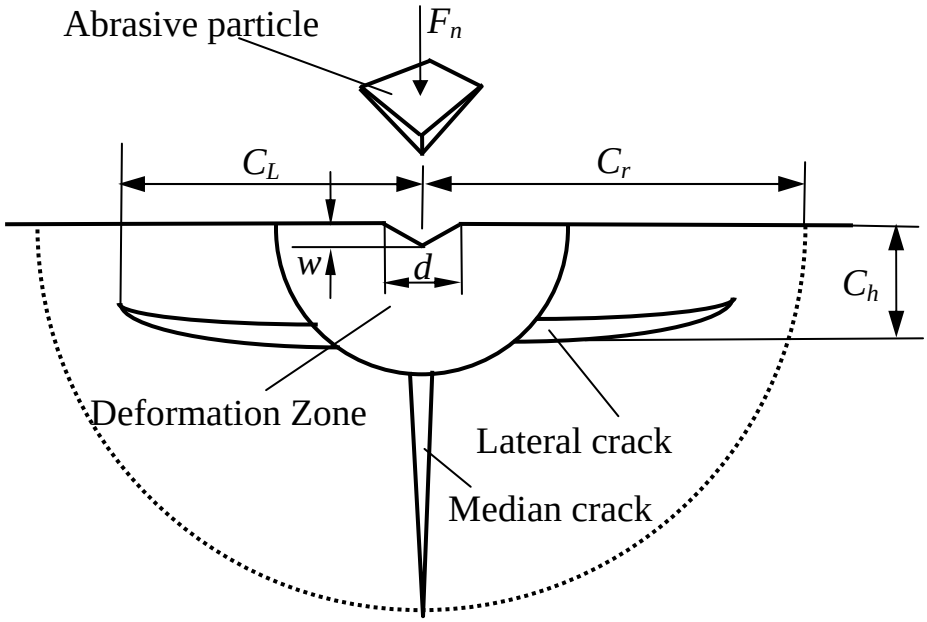

Fig. 4. Cracks in brittle material induced by indentation of an abrasive particle (after [27]).

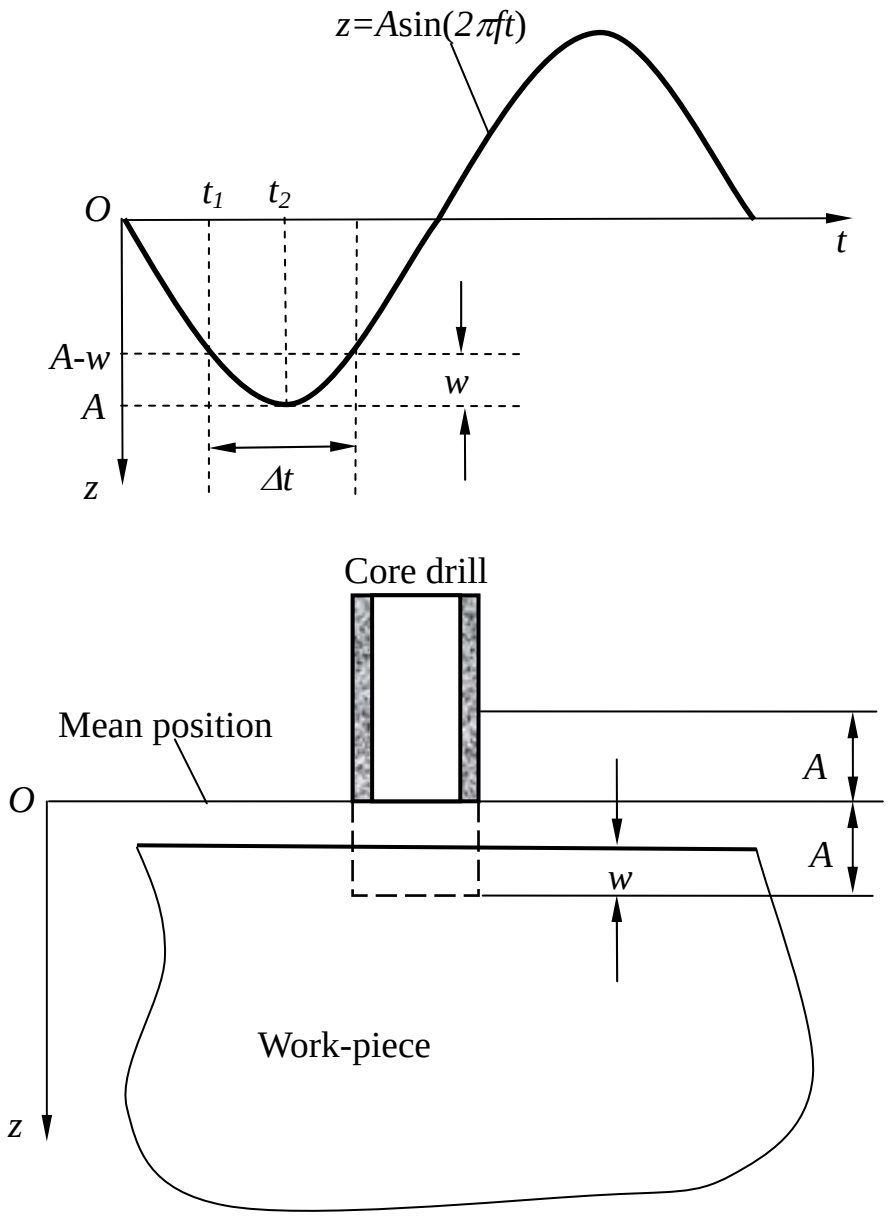

Fig. 5. Calculation of effective cutting time Δt (after [14]).

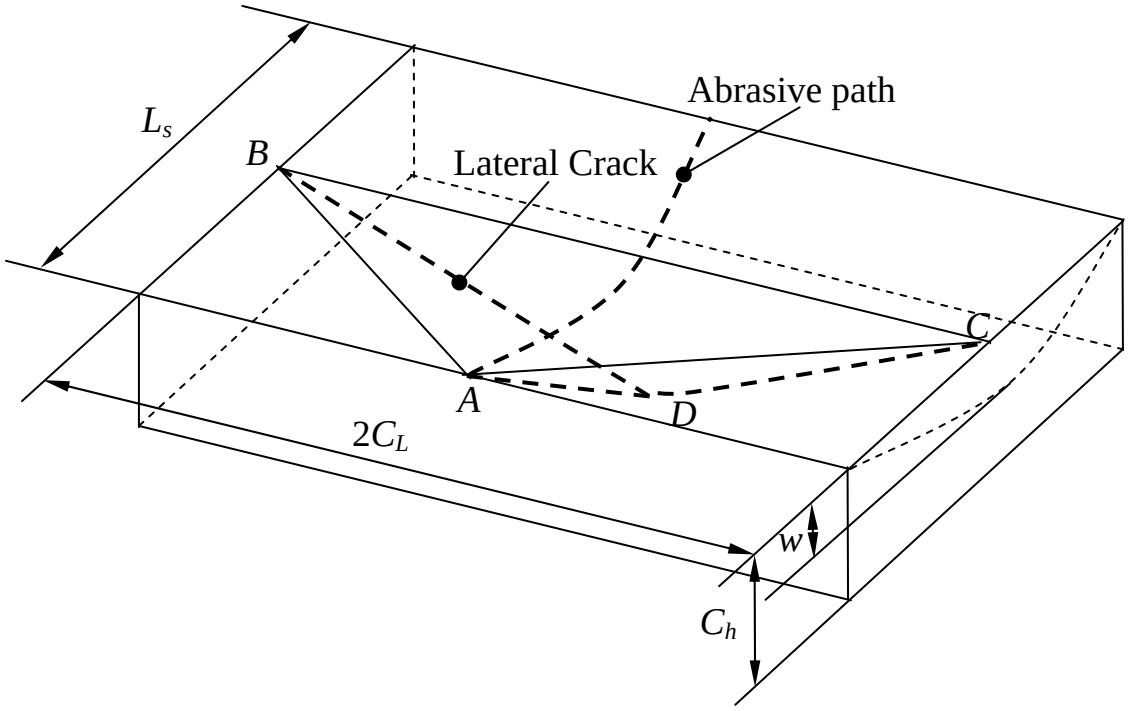

Fig. 6. Calculation of theoretical volume (V_0) of fracture zone.

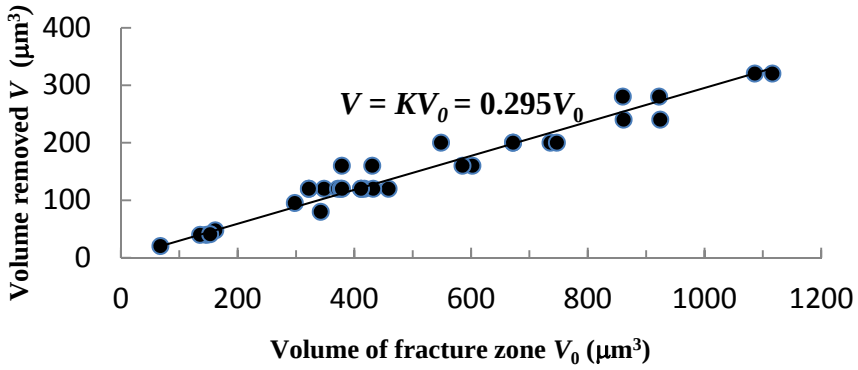

Fig. 7. Calculation of *K* from experimental data.

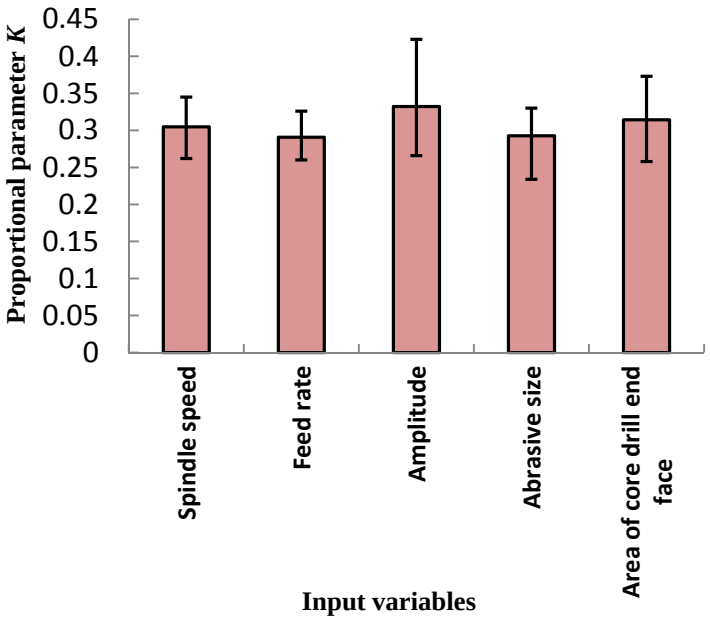
Proportional parameter K
0.45
0.4
0.35
0.3
0.25
0.2
0.15
0.1
0.05
0
Spindle speed
Feed rate
Amplitude
Abrasive size
Area of core drill end face
Input variables

(a)

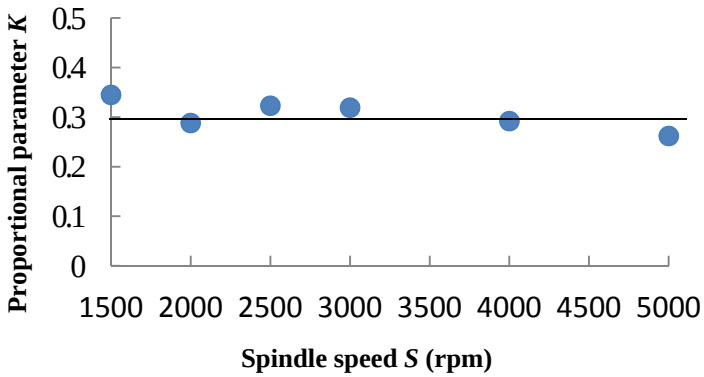
Proportional parameter K
0.5
0.4
0.3
0.2
0.1
0
1500 2000 2500 3000 3500 4000 4500 5000
Spindle speed S (rpm)

(b)

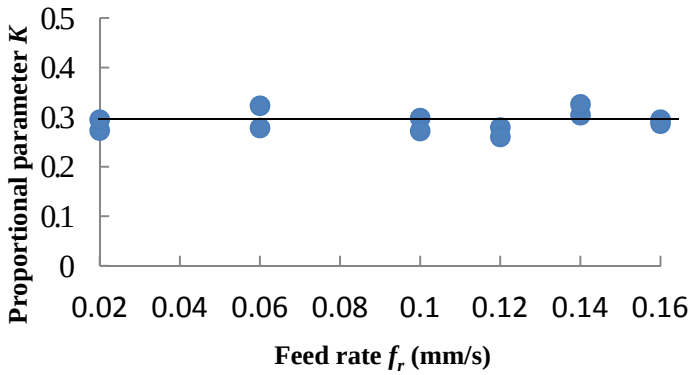
Proportional parameter K
0.5
0.4
0.3
0.2
0.1
0
0.02 0.04 0.06 0.08 0.1 0.12 0.14 0.16
Feed rate f_r (mm/s)

(c)

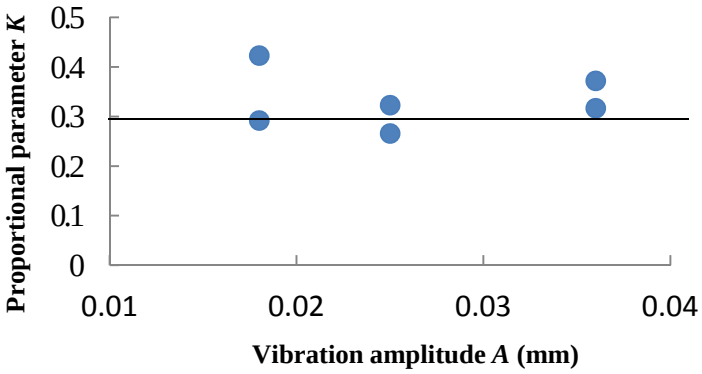

(d)

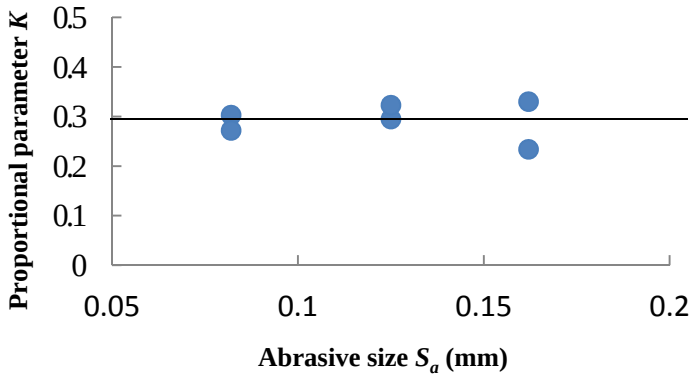

(e)

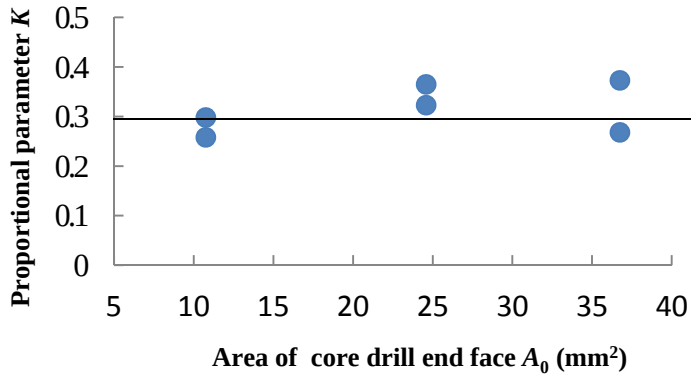

(f)

Fig. 8. Influences of input variables on *K*.

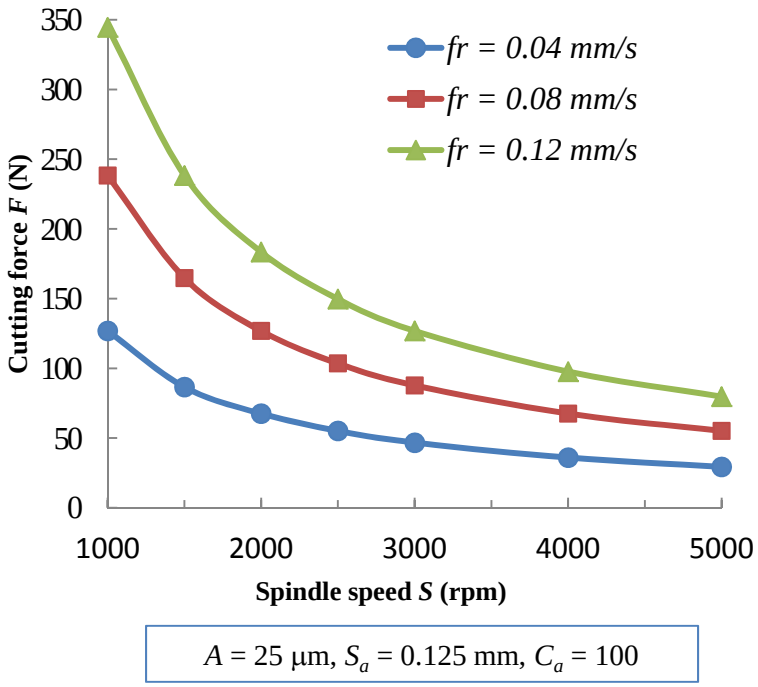

Fig. 9. Predicted relation between cutting force and spindle speed.

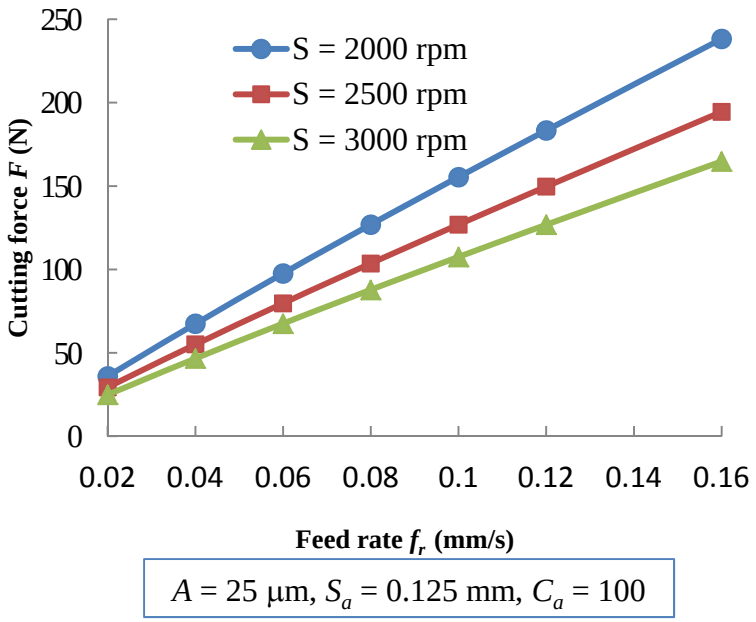

Fig. 10. Predicted relation between cutting force and feed rate.

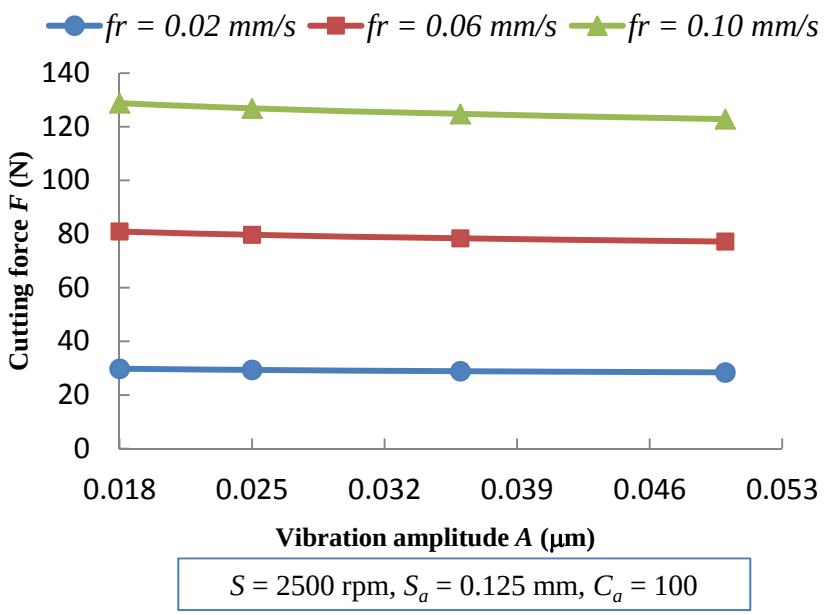

Fig. 11. Predicted relation between cutting force and vibration amplitude.

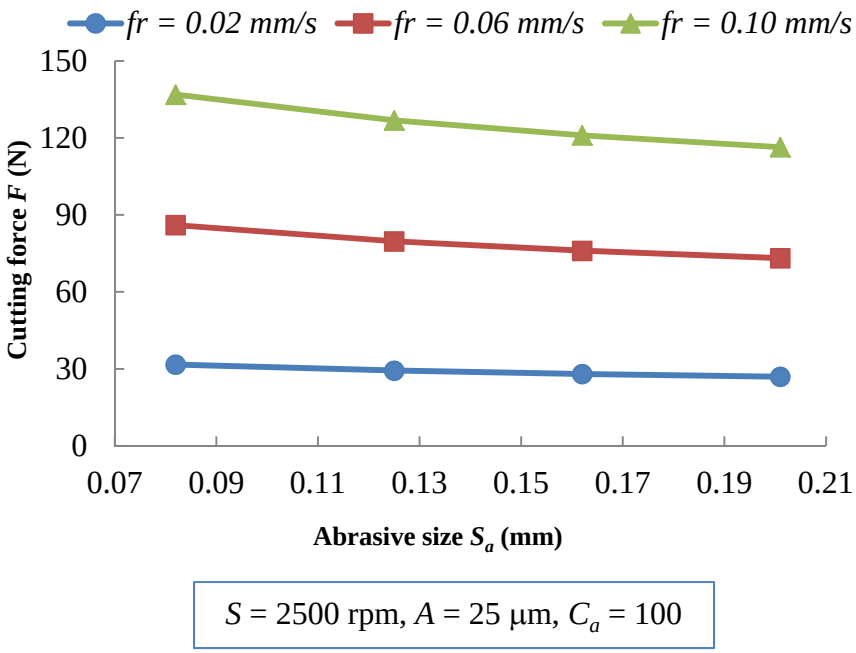

Fig. 12. Predicted relation between cutting force and abrasive size.

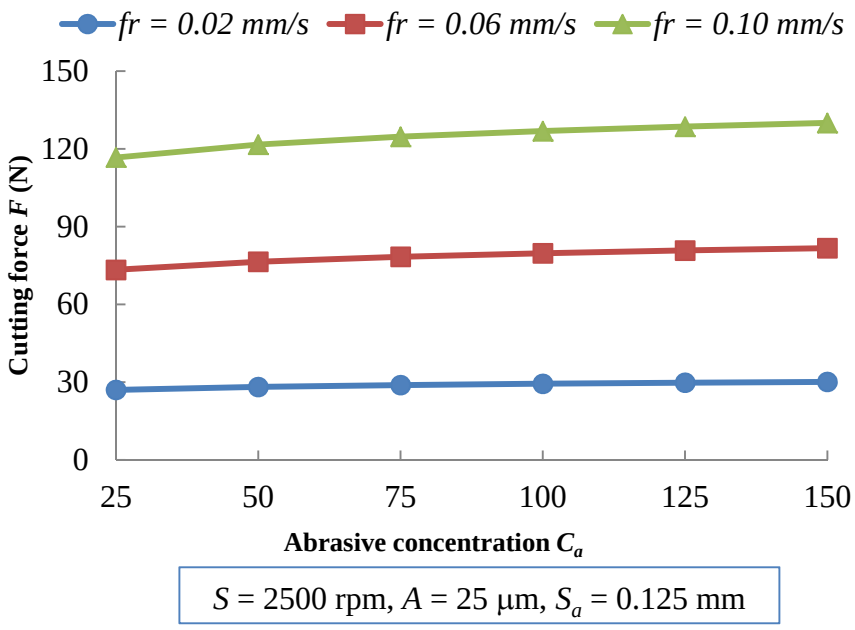

Fig. 13. Predicted relation between cutting force and abrasive concentration.

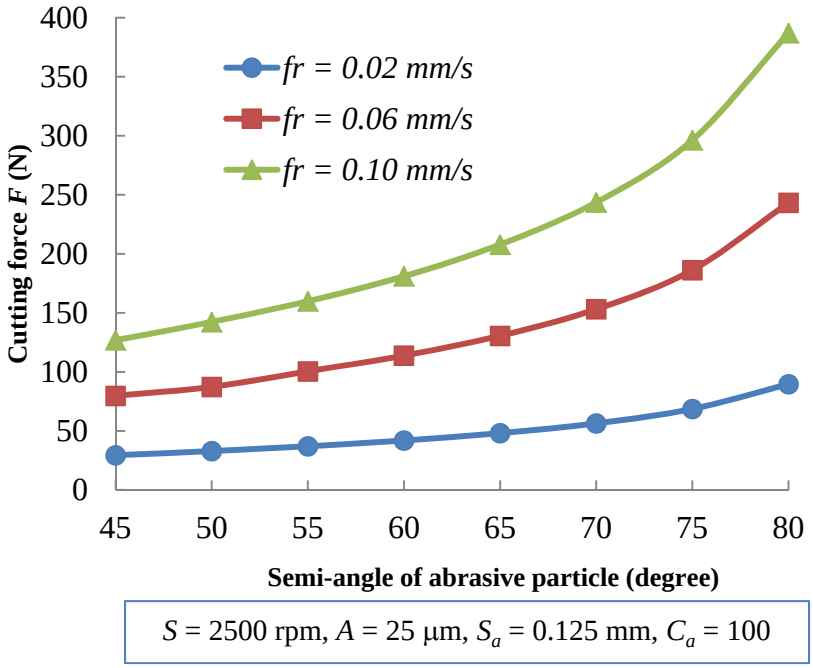

Fig. 14. Predicted relation between cutting force and semi-angle of abrasive particle.

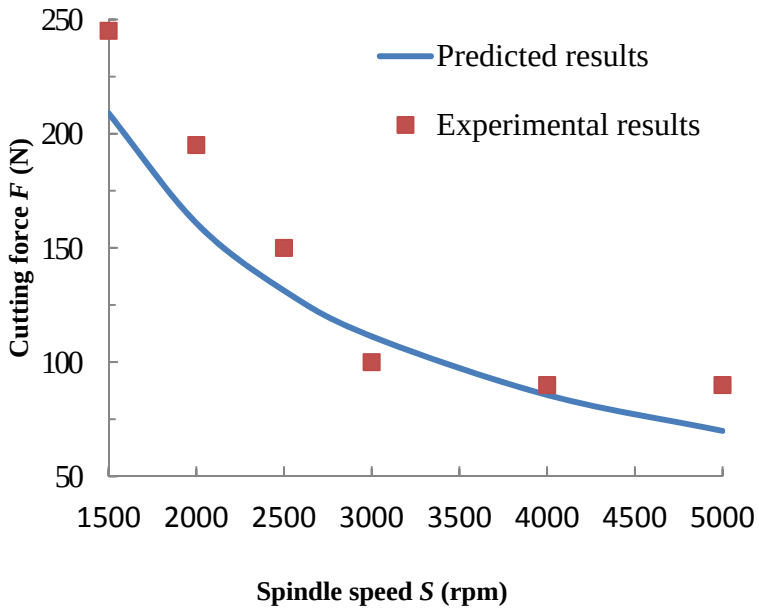

(a)

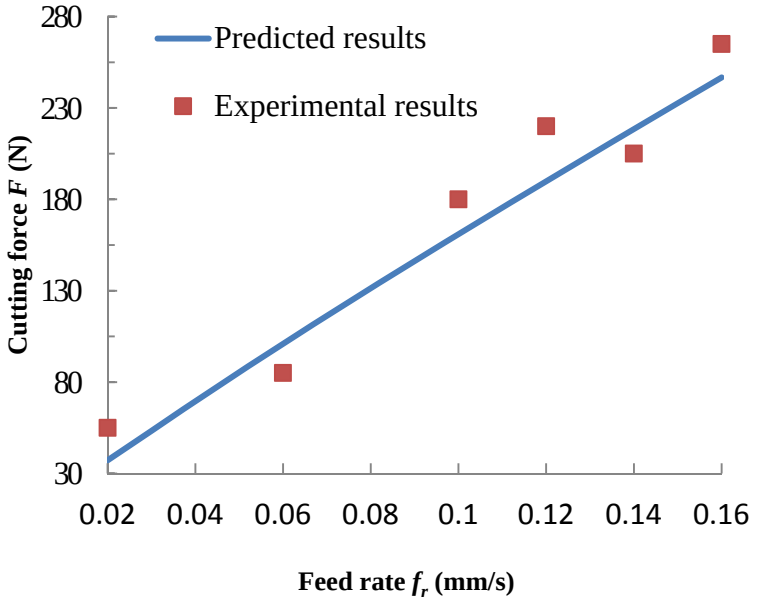

(b)

Fig. 15. Comparison of cutting force between predicted results and experimental results. (a) f_r = 0.1 mm/s, (b) S = 2000 rpm.

Table 1

Identifications of core drills used in experiments

Drill ID	Mesh size	Abrasive size S_a (mm)	Abrasive concentration C_a	Outer Diameter D_o (mm)	Inner Diameter D_i (mm)
1	#80-100	0.162	100	9.6	7.8
2	#180	0.082	100	9.6	7.8
3	#100-120	0.125	100	9.6	7.8
4	#80-100	0.162	100	5.08	3.48
5	#80-100	0.162	100	12.7	10.7
6	#60-80	0.201	100	12.7	10.7

Table 2

Experimental conditions for obtaining K

Experiment	Spindle speed S (rpm)	Feed rate f_r (mm/s)	Vibration amplitude A (mm)	Drill ID
1st group	1500, 2000, 2500, 3000, 4000, 5000	0.06	0.025	No. 1
2nd group	2500	0.02, 0.06, 0.10, 0.12, 0.14, 0.16	0.025	No. 1
3rd group	2500	0.06, 0.08	0.018, 0.025, 0.036	No. 1
4th group	2500	0.04, 0.08	0.025	No. 1, 2, 3
5th group	2500	0.06, 0.10	0.025	No. 1, 4, 5

Table 3

Conditions for pilot experimental verification

Input variable	Value
Spindle speed S (rpm)	1500, 2000, 2500, 3000, 4000, 5000
Feed rate f_r (mm/s)	0.02, 0.06, 0.10, 0.12, 0.14, 0.16
Vibration amplitude A (mm)	0.032
Core drill ID	No. 6